LA-UR- 08-6889

Approved for public release; distribution is unlimited.

Title:	Melting of defective Cu with stacking faults
Author(s):	Li-Bo Han, Qi An, Rong-Shan Fu, University of Science & Technology of China; Lianqing Zheng, Florida State University; Shengnian Luo, LANL
Intended for:	Journal of Chemical Physics

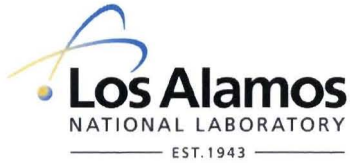

Form 836 (7/06)

Submitted to *Journal of Chemical Physics*

Melting of defective Cu with stacking faults

Li-Bo Han, Qi An,* and Rong-Shan Fu
School of Earth and Space Sciences, University of Science and Technology of China, Hefei, Anhui 230026, P.R. China

Lianqing Zheng
School of Computational Science, Florida State University, Tallahassee, FL 32306, USA

Sheng-Nian Luo†
Physics Division, Los Alamos National Laboratory, Los Alamos, NM 87545, USA
(Dated: October 13, 2008)

We conduct classical molecular dynamics simulations to investigate isobaric melting of defective Cu solids with only one type of defect: intrinsic or extrinsic stacking faults. We characterize bulk melting and nucleation of melt in terms of order parameters, liquid cluster analysis and the mean-first-passage-time method. The stacking faults induces negligible reduction in the temperature at melting, and the amount of superheating in these defective solids is the same as the perfect solids. Both homogeneous and heterogeneous nucleation of melt are observed; the existence of the stacking faults only slightly increases the nucleation rate and the probability of nucleation at heterogeneous nucleation sites. Such observations can be attributed to the low energy of the stacking faults and the extremely high heating rates in molecular dynamics simulations. These results underscore the necessity of considering the effects of rate and defect when interpreting experimental and simulation results as regards, e.g., phase boundaries.

I. INTRODUCTION

Defects are ubiquitous in real solids, and affect phase transitions in various manners.[1] For example, defects normally lower the melting temperature. Noticeable progresses have been made recently on melting of perfect solids including superheating and homogeneous nucleation.[2–4] Nonetheless, melting of defective solids is much more complicated; the related phenomena are extremely rich and remain to be revealed, and the physics behind, to be understood.

Defects include vacancies, voids, dislocations, stacking faults, grain/phase boundaries, and free surfaces. To better understand melting of defective solids, it is desirable to study individual defects first since various defects intact with each other during heating and melting processes. Previous simulation efforts along this line have focused on the melting phenomena of solids with voids, free surfaces (clusters) and grain boundaries.[5–8] Here, we perform classical molecular dynamics (MD) simulations on a representative solid (Cu) to examine a single defect type in face-centered-cubic (fcc) solids, stacking faults. This study is also motivated by previous experimental works that claim the important role of the stacking faults in melting.[9,10] Since first-order phase transitions such as melting are rate dependent, MD simulations with accurate interatomic potentials and high heating rates serve as unique complements to low heating rate experiments as well. Our work shows that stacking faults have only limited effects on bulk melting and nucleation owing to the extremely high heating rates in conventional MD simulations and the low energy of the stacking faults. Sec. II describes the methodology in constructing the intrinsic and extrinsic stacking faults, and MD simulations and analyses. The results and discussion are presented in Sec. III, followed by summary and conclusion in Sec. IV.

II. METHODOLOGY

In fcc metals such as Cu, the regular sequencing of the close-packed {111} planes is *ABC*... An interruption to this sequencing, e.g., *ABCABABC* or *ABCABACABC*..., results in either intrinsic or extrinsic stacking fault, respectively (Fig. 1). An intrinsic stacking fault (ISF) can be produced via a sliding process. Sliding of one part of an fcc crystal over another across a {111} plane in the $[\bar{2}11]$ direction yields a (general) stacking fault.[11] For a given slide distance, we relax the defective crystal with the conjugate gradient method to minimize its potential energy. A tabulated embedded atom method (EAM) potential[12] is adopted to describe the atomic interactions in Cu and for energy minimization. The extra energy per unit area of the stacking fault, γ, is then calculated as a function of fault translation vector ($\mathbf{d}$),[11] and agrees with an independent calculation using the same potential[12] (Fig. 2). The nonzero local minima of $\gamma(\mathbf{d})$, e.g., at $\mathbf{d} = \frac{1}{6}[\bar{2}11]$ (1.475 Å), represent the intrinsic stacking faults (metastable) with an energy $\gamma_{\rm ISF} \approx 44$ mJ/m^2. For the extrinsic stacking fault, an extra {111} layer is inserted into the regular sequencing; similar energy minimization is applied to the defective crystal and the extrinsic stacking fault energy is nearly identical to $\gamma_{\rm ISF}$.

We characterize the relaxed configurations with the intrinsic ($\mathbf{d} = \frac{1}{6}[\bar{2}11]$) and extrinsic stacking faults in terms of order parameters (see below). While the atomic coordination numbers remain unchanged, the order parameters of the atoms in the four or five {111} layers around the stacking faults (dotted lines, Fig. 1) are reduced from

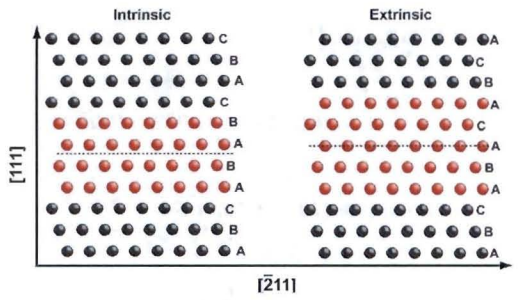

FIG. 1: Atomic configurations of intrinsic and extrinsic stacking faults in fcc Cu. Dashed lines refer to the stacking faults.

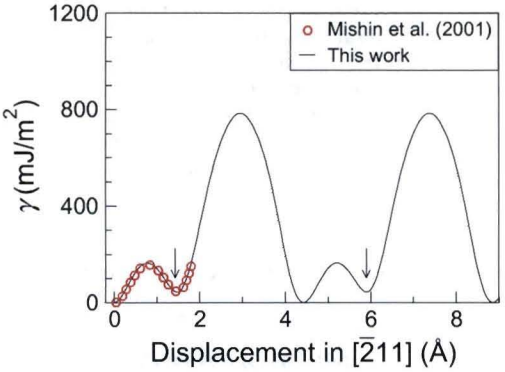

FIG. 2: Stack fault energy γ of Cu as a function of the translation vector $\mathbf{d}$ during sliding across $\{111\}$. The arrows indicate the intrinsic stacking faults.

1 to 0.74–0.92. The number of $\{111\}$ layers affected by a stacking fault, or its thickness, is thus four and five for the intrinsic and extrinsic stacking faults, respectively. The reduced ordering and elevated free energy associated with the stacking faults may enhance the probability of melt nucleation around them.

MD simulations are performed on the relaxed defective crystals with the same EAM potential for energy minimization. A constant-pressure-temerature ensemble and three-dimensional periodic boundary conditions are applied. Temperature (T) is controlled with a Hoover thermostat,[13] and the isotropic pressure, with isotropic volume scaling.[14] The solids undergo incremental heating into liquid regime at ambient pressure, and the temperature increment is 20 K at high temperatures. The time step for integrating the equation of motion is 1 fs. At each temperature, the run duration is 50 ps. For simulations with intrinsic stacking faults, the system size is mostly 90240 atoms, and a large system with over 10^6 atoms is also explored. The system size is 95000 atoms in the case of extrinsic stacking fault.

To quantify local and global structure disordering, we calculate the local order parameters of individual atoms and the global order parameter of the whole system.[15] We choose a set of $N_{\mathbf{q}} = 6$ direction vectors $\{\mathbf{q}\}$ satisfying $\exp(i\mathbf{q}\cdot\mathbf{r}) = 1$, for vectors $\{\mathbf{r}\}$ connecting an atom and its neighbors in a perfect fcc solid. The local order parameter of a specific atom is defined as

$$\psi = \left| \frac{1}{N_{\mathbf{q}}} \frac{1}{N_c} \sum_{\mathbf{r}} \sum_{\mathbf{q}} \exp(i\mathbf{q}\cdot\mathbf{r}) \right|^2 , \qquad (1)$$

where N_c is the coordination number, and vector $\mathbf{r}$ refers to the atom and its nearest neighbors in an (defective) fcc solid or its melt under consideration. The first minimum distance in the radial distribution function (RDF) is taken as the nearest-neighbor distance. ψ is essentially a local static structure factor. Averaging ψ among an atom and its N_c nearest neighbors yields an averaged local order parameter of this atom, $\bar{\psi}$, which is used for characterizing local disordering. The global order parameter (Ψ) is the average of ψ over all the atoms in the system.

III. RESULTS AND DISCUSSION

A heated solid melts with sharp changes in such physical properties as enthalpy, density and global ordering as expected for first order phase transitions. Fig. 3 is an example of the evolution of the global order parameter as a function of temperature. In the case of intrinsic stacking fault, Ψ decreases gradually from ~0.94 at 300 K to 0.44 at 1600 K, and then drops rapidly to 0.066 upon melting at 1620 K; Ψ evolves in a nearly identical manner in the case of extrinsic stacking fault. Melting is also identified at 1620 K from the evolutions of enthalpy and density during heating of the defective solids with intrinsic or extrinsic stacking faults. However, the equilibrium (thermodynamic) melting temperature for Cu as predicted by this EAM potential is about 1325 K.[2] Appreciable superheating (22%) still occurs even in the presence of these stacking faults.

We examined previously in detail the melting process of perfect Cu single crystals described by the same EAM potential, and found that the solids melt at the maximum superheating temperature of 1620 K. This superheating temperature is identical to that for the defective solids with intrinsic or extrinsic stacking faults (the uncertainty is approximately an temperature increment, 20 K). Contrary to conventional wisdom, the defective solids with the stacking faults melt at a superheated state rather than near the equilibrium melting temperature; the reduction of superheating due to these defects is not detectable within simulation uncertainties and premelting is certainly absent.

We also compute the global order parameters as a function of time (t) during melting of the defective solids at 1620 K. $\Psi(t)$ is similar in the cases of the intrinsic and extrinsic stacking faults (Fig. 4), and the perfect solid melted at the same temperature[2] (not shown): Ψ decreases from about 0.4 at solid state to 0.115 at liquid state within about 10 ps. However, the onset of melting

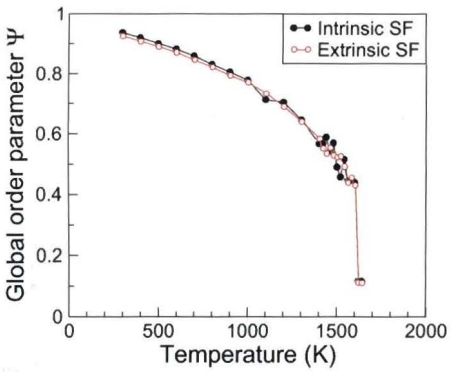

FIG. 3: Global order parameter as a function of temperature for the defective Cu solids and their melts. SF: stacking fault.

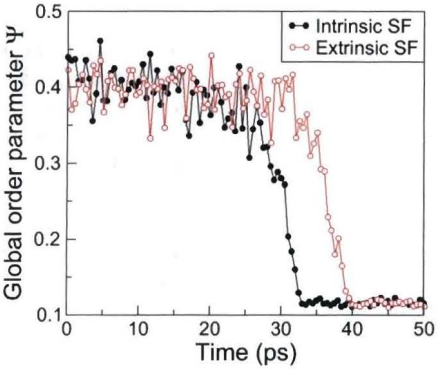

FIG. 4: Temporal evolution of the global order parameter during melting at 1620 K, for the defective solids with stacking faults (SF).

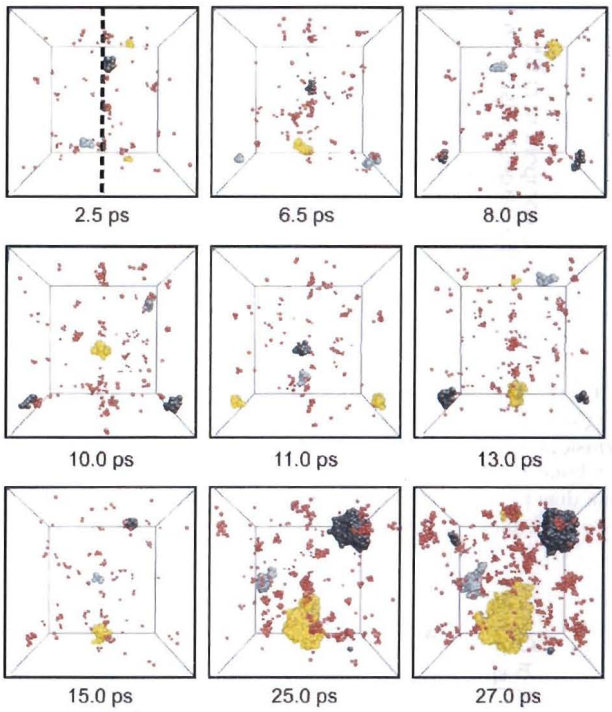

FIG. 5: Configurations of liquid atoms during melting at 1620 K. Color coding refers to the liquid cluster size. Atoms in the first, second and third largest clusters are colored yellow, black and gray, respectively; the rest are colored red. The dashed line (2.5 ps) denotes the nominal position of the intrinsic stacking faults.

is different, since crossing the energy barrier for melting is caused by fluctuations and thus stochastic in nature.[2,16]

Although negligible (or small) effects of the stacking faults are detected on the bulk melting behavior, it would still be interesting to examine nucleation of melt, e.g., homogeneous versus heterogeneous nucleation. To characterize the melt nucleation and growth process at atomistic scales, we conduct time-resolved cluster analysis of the liquid atoms[2] based on the atomic configurations obtained at 1620 K, taking the intrinsic stacking faults as example. (The liquid atoms refer to the atoms with $\bar{\psi} \leq 0.115$; see Figs. 3 and 4.) Two atoms belong to the same cluster or nucleus if they are within the nearest-neighbor distance (obtained from RDF) of each other. Liquid cluster distributions at different instants during melting at 1620 K are illustrated in Fig. 5 for a single run. (Visualization adopted AtomEye.[17]) Nucleation of liquid nuclei occurs near and off the stacking fault, indicating both heterogeneous and homogeneous nucleation. A nucleus may disappear and its size fluctuates drastically until it is stabilized in location and grows rapidly. In this particular case shown in Fig. 5, the largest, stabilized cluster is located within the stacking fault.

The largest cluster is key to melting since its growth after stabilization in location dominates smaller nuclei, and the bulk melting can only be observed after this point. (A stabilized nucleus is actually supercritical in size, i.e., larger than the critical size.[2]) We thus follow its location (center of mass, CM) during the course of melting, as shown illustratively in Fig. 6 for two runs (A and B). We only plot the z-component since the z-axis is normal to the stacking fault. The location evolves in two stages, pronounced fluctuation (stage I) and stabilization (stage II). In stage I, the largest nucleus appears either near or off the stacking faults since the maximized chemical driving force at the extreme superheating allows both heterogeneous and homogeneous nucleation to be observed in MD time scales. Run A shows pronounced fluctuations and the cluster becomes stabilized near the stacking fault, and the opposite occurs for run B.

In order to investigate the probability, p_1, that the largest nucleus becomes stabilized near the stacking fault, we conduct 50 independent runs on a system of 90240 atoms (47 {111} layers) with intrinsic stacking faults at 1620 K. Each run is started with a different random number seed for velocity assignment but with the same initial configuration, and pressure and temperature controls. Using the same liquid cluster analysis as shown

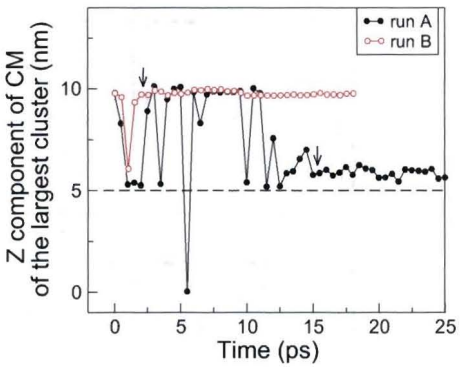

FIG. 6: Temporal evolutions of the center of mass of the largest liquid cluster for melting of defective solids with intrinsic stacking faults at 1620 K. Two separate runs are shown for homogeneous and heterogeneous nucleation. The dashed line denotes the nominal position of the stacking faults. The arrows define stages I and II (see text).

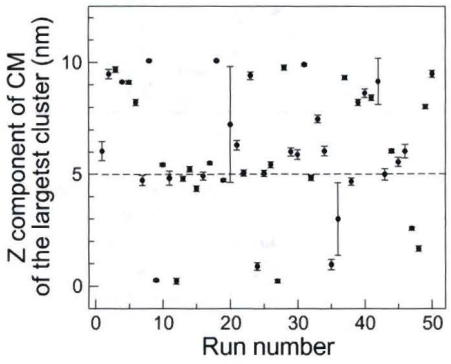

FIG. 7: Center of mass of the largest stabilized liquid cluster for 50 independent runs. Also see Fig. 6.

above, we obtain the location of the largetst cluster in each run (Fig. 7). The thickness of stacking fault is 4 (1.04 nm), and its volume fraction in the whole system is about 0.09. A run is counted for p_1 if the largest cluster in stabilized within this thickness. The apparent value of p_1 is thus about 18/50=0.36. After correction for the volume fraction, $p_1 \sim 0.86$.

The nucleation rate of the critical nuclei can be characterized with the mean-first-passage-time (MFPT) method[16,18] as detailed in Refs.[2,16]. The MFPT (τ) is defined as the instant when the size of the largest nucleus reaches or exceeds a given size $n_{\max}$ for the first time, and its value is obtained by averaging 50 statistical runs (Fig. 8). The nucleation rate J and the critical nucleation size n^* can be deduced via fitting to $\tau(n_{\max})$ with

$$\tau(n_{\max}) = \frac{\tau_J}{2}\{1 + \mathrm{erf}\,[(n_{\max} - n^*)c]\}, \qquad (2)$$

where τ_J, n^* and c are fitting parameters. Then, $J = 1/(\tau_J V)$ where V denotes the solid volume under consideration. The $n_{\max}$ curve is sigmoidal but does not reach

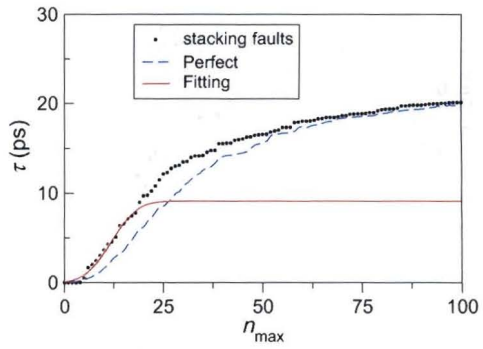

FIG. 8: The mean-first-passage-time (τ) versus the largest liquid cluster size ($n_{\max}$) in the case of intrinsic stacking faults, compared to melting of a perfect Cu solid. Fitting refers to Eq. (2).

a well defined plateau. This indicates that the growth of a critical nucleus occurs at similar time scales as its nucleation,[16] i.e., nucleation is coupled with growth due to the low energy barrier at the extreme of superheating. In such cases, Eq. (2) is still valid.[16] The fitting yields $\tau_J = 9.1$ ps and $n^* = 11.7$. In the case of the stacking faults, τ_J and n^* are smaller than 13.9 ps and 21.6, respectively, obtained in melting of a perfect solid[2] (Fig. 8); however, $J \approx 9.2 \times 10^{34}$ s^{-1}m^{-3}, slightly higher than (or similar to) that in the latter case (9×10^{34} s^{-1}m^{-3}).[2]

The run with the larger system (>10^6 atoms) shows similar behavior in bulking melting and nucleation, except that a stabilized nucleus forms at 1600 K rather than 1620 K. The largest nucleus is stabilized outside the stacking fault thickness. Statistical runs are not performed because of current computational limitations but we expect that the runs on the smaller system ($\sim 10^5$ atoms) are sufficiently representative.

The stacking faults by themselves appear to have small or negligible effect in reducing the melting temperature, and the related bulk melting is similar to that in the perfect solid. This is consistent with the observation that the shapes of the growing, stabilized (supercritical) liquid nuclei are similar in homogeneous and heterogeneous nucleation sites, i.e., the nuclei centered within the stacking fault do not take its shape (Fig. 5). Superheating is largely dictated by the heating rate (time scale) and the effective energy barrier to melting.[1,4,19] The latter can be lowered by the existence of defects; thus defects act to offset the effect of heating rate on superheating. At the extreme heating rate as in conventional MD simulations, the heating rate effect outruns the reduction in the energy barrier by the low energy stacking faults. As a first order comparison, γ_{ISF} (46 mJ/m^2) is only about 25% of the solid–liquid interfacial energy (177 mJ/m^2).[2] The volume fraction of the stacking faults ($\sim$0.1) is already much higher than those in normal solids, but we expect that increasing the volume fraction of the stacking faults may induce a noticeable reduction in the temperature at melting.

The low energy stacking faults enhances the (normalized) probability of the nuclei stabilized within the stacking faults from 0.5 to 0.85 in our simulations. Such an increase is actually very limited since the nucleation rate is an exponential function of the energy barrier,[1] thus consistent with stacking fault's small effect on the bulk melting behavior. Another consistent observation is that, the nucleation rate of the critical nuclei in the case of the stacking faults is only slightly higher than that in melting of a perfect Cu solid. The low energy of the stacking faults and the extremely high heating rates are the causes.

Stacking faults were invoked as the main cause of the appreciable lowering in the slope of the high pressure melting curve (dT/dP; P denotes pressure) in diamond anvil cell experiment on Xe.[10] However, the effects of stacking faults are small in our simulations. One explanation is the possible existence of nonhydrostaitcity during compression-heating which may have increased the density of stacking faults by several orders of magnitude, thus reducing the apparent (not necessarily thermodynamic) melting temperature. Another is the slow heating rate in such experiments compared to MD simulations ($\sim$1 K/s versus 10^{11} K/s); heterogeneous nucleation plays a more important, possibly dominant, role at low heating rates and its effect decreases with increasing heating rate and chemical driving force.[19] Thus, when comparing simulation and experimental results as regards first-order phase transitions and thermodynamic phase boundaries, it is important to consider the rate effect and low energy defects such as stacking faults.

IV. CONCLUSION

We have performed MD simulations to examine isobaric melting of defective Cu solids with intrinsic or extrinsic stacking faults, including bulk melting and nucleation. The defective solids show similar bulk melting to the perfect solids, i.e., the stacking faults have small or negligible effects on the bulk melting at such high heating rates. Both homogeneous and heterogeneous nucleation occur; the stacking faults only slightly increase the nucleation rate and the probability of the largest liquid nucleus being stabilized at heterogeneous nucleation sites. These results can be explained by the extremely high heating rates in the conventional MD simulations and the lower energies of the stacking faults. The effects of heating rate and defects should be considered for a meaningful comparison as regards phase boundaries among various experiments and simulations.

Acknowledgments

L.B.H. and Q.A. acknowledge the support from NSF of China Grants No. 40537033 and 40425005. L.Z. is grateful for W. Yang's support. S.N.L. was partially supported by the Laboratory Directed and Research Development program at LANL. LANL is under the auspices of U.S. Department of Energy under contract No. DE-AC52-06NA25396.

* Present address: Materials and Process Simulation Center, California Institute of Technology, Pasadena, CA 91125, USA.

† Electronic address: sluo@lanl.gov

[1] J. W. Christian, *The Theory of Transformation in Metals and Alloys* (Pergaman, New York, 1965).

[2] L. Q. Zheng, Q. An, Y. Xie, Z. H. Sun, and S. N. Luo, J. Chem. Phys. **127**, 164503 (2007).

[3] Z. H. Jin, P. Gumbsch, K. Lu, and E. Ma, Phys. Rev. Lett. **87**, 055703 (2001).

[4] S. N. Luo, T. J. Ahrens, T. Çağın, A. Strachan, W. A. Goddard III, and D. C. Swift, Phys. Rev. B **68**, 134206 (2003).

[5] J. D. Honeycutt and H. C. Andersen, J. Phys. Chem. **91**, 4950 (1987).

[6] P. M. Agrawal, B. M. Rice, and D. L. Thompson, J. Chem. Phys. **119**, 9617 (2003).

[7] S. J. Zhao, S. Q. Wang, T. G. Zhang, and H. Q. Ye, J. Phys.: Condes. Matter **34**, L549 (2000).

[8] S. N. Luo, L. Q. Zheng, and O. Tschauner, J. Phys.: Condens. Matter **18**, 659 (2006).

[9] S. Link, Z. L. Wang, and M. A. El-Sayed, J. Phys. Chem. B **104**, 7867 (2000).

[10] R. Boehler, M. Ross, P. Soderlind, and D. B. Boercker, Phys. Rev. Lett. **86**, 5731 (2001).

[11] V. Vitek, Phil. Mag. **18**, 773 (1968).

[12] Y. Mishin, M. J. Mehl, D. A. Papaconstantopoulos, A. F. Voter, and J. D. Kress, Phys. Rev. B **63**, 224106 (2001).

[13] W. G. Hoover, Phys. Rev. A **31**, 1695 (1985).

[14] J. Stadler, R. Mikulla, and H.-R. Trebin, Int. J. Mod. Phys. C **8**, 1131 (1997).

[15] J. R. Morris and X. Song, J. Chem. Phys. **116**, 9352 (2002).

[16] J. Wedekind, R. Strey, and D. Reguera, J. Chem. Phys. **126**, 134103 (2007).

[17] J. Li, Modell. Simul. Mater. Sci. Eng. **11**, 173 (2003).

[18] P. Hänggi, P. Talkner, and M. Borkovec, Rev. Mod. Phys. **62**, 251 (1990).

[19] Z. P. Tang, *Shock-Induced Phase Transitions* (Science Press, Beijing, 2008).